Molecular Dynamics Investigation of ^{23}Na NMR Relaxation in Oligomeric DNA Aqueous Solution

Francesca Mocci,[†] Aatto Laaksonen,[‡] Alexander Lyubartsev,[‡] and Giuseppe Saba*[,†]

Dipartimento di Scienze Chimiche, Universita' di Cagliari, Cittadella Universitaria di Monserrato, I-09042 Monserrato (Cagliari), Italy, and Division of Physical Chemistry, Arrhenius Laboratory, Stockholm University, S-106 91 Stockholm, Sweden

Received: May 25, 2004; In Final Form: August 5, 2004

An 8 ns molecular dynamics (MD) simulation has been carried out on an oligomeric DNA duplex in a minimal salt sodium aqueous solution in order to study the magnetic relaxation process of ^{23}Na. The explicit modeling of the solvent and the time length of the simulation allow study of the fast and, to some extent, the slow components of the relaxation. In agreement with experimental studies of the quadrupolar relaxation of monatomic cations in oligomeric DNA solution, the relaxation displays a multiexponential decay. According to the simulation, the slow components originate from ions directly bound to the DNA surface. The effects of the binding of the cations to DNA on the static and dynamical relaxation parameters have been studied in different binding sites either in the grooves or in the backbone. This study reveals that the quadrupolar coupling constant and the spectral densities vary largely from site to site, the fastest relaxation occurring for the ion directly bound to the minor groove. The combination of MD results with quadrupolar relaxation experimental data suggests that the occupancy of the binding sites in the minor groove of uninterrupted adenine sequences is relatively low.

1. Introduction

The nuclear magnetic relaxation of spin $I > {}^1/_2$ nuclei occurs mainly through the coupling of the nuclear electric quadrupole moment and the electric field gradient at the nuclear site, originated by the nearby charge distributions. For atomic ions such as ^{23}Na, $I = {}^3/_2$, in simple aqueous solution or associated with polyelectrolytes, the coupling depends both on the symmetry of the charge distribution and on the fluctuations of the electric field gradient. Therefore measuring the nuclear spin relaxation rate can provide useful information about the microscopic dynamics of the nucleus and its environment. In fact, the ^{23}Na nuclear spin relaxation has been used to investigate, among others, the interactions of counterions with DNA and their effects on the structural and dynamical properties of DNA both in the native state and in association with different classes of DNA binders.[1−5]

Recently great interest has been devoted to the study of the direct binding of monovalent counterions to DNA, both in the solid state and in solution, by means of X-ray crystallography,[6−11] NMR,[12,13] and molecular dynamics.[14−25] These studies revised the common view of monovalent cations binding to the DNA double helix in a delocalized manner, without dehydration and irrespective of the base sequence.[2] As a matter of fact, an ad hoc designed ^{23}Na nuclear magnetic relaxation dispersion (NMRD) experiment assessed the sequence specificity of the direct binding of monatomic monovalent counterions.[13]

Despite the wide application of ^{23}Na NMR to study the dynamics of DNA and its interaction with other molecules, several microscopical aspects of the dynamics of the electric field gradient experienced by the quadrupolar nuclei in DNA solution have to be clarified as yet. In particular, little is known on the influence of differently bound sodium ions on the NMR quadrupolar relaxation and on the form of the underlying spectral density functions.

Since the time constants characterizing the ^{23}Na magnetization decay in a macroscopically isotropic DNA solution range from the subpicosecond to the nanosecond time scale, the use of molecular dynamics (MD) simulation is potentially a powerful method to obtain information at the microscopic level on the NMR relaxation processes.

This technique has provided deep and useful insights into the mechanism of spin relaxation of ions and noble gases in solution, often leading to values of the NMR observables in good agreement with the experimental data (see Odelius and Laaksonen[26] for a recent review); however to our knowledge only a few investigations have studied the quadrupolar nuclear spin relaxation of ^{23}Na in polyelectrolyte solution.[27−30]

In the present work, we report on an atomistic MD study of the fluctuations of the electric field gradient at the sodium nuclei in an aqueous solution of the DNA duplex CT_4A_4G. This oligomer comprises two uninterrupted adenine sequences (A-tracts) linked by a 5′-TA-3′ step. A-tracts are known to possess a narrow minor groove, compared to the canonical B-DNA, which widens at the TA steps. The occurrence of these structural features makes this sequence a good model for studying the effects on the ^{23}Na quadrupolar relaxation of ion binding to the minor groove of A-tracts, which lately has been the subject of numerous studies,[6,7,10,12,13,19,21,22,25] without excluding other kinds of interactions which can take place in the larger minor groove at the center of the oligomer.

* To whom correspondence should be addressed. E-mail: pino@nmr.unica.it.
[†] Universita' di Cagliari.
[‡] Stockholm University.

10.1021/jp047744+ CCC: $27.50
Published on Web 09/21/2004

2. Theory

The return to thermal equilibrium of the ^{23}Na transverse and longitudinal magnetizations is known to be biexponential;[31] the four relaxation rates are related to the electric field gradient (EFG) at the nucleus via the spectral densities $J(\omega)$. In isotropic solutions, they are given by the following equations:

$$R_{1f} = 2\left(\frac{eQ}{\hbar}\right)^2 J_{00}(\omega_0)$$

$$R_{1s} = 2\left(\frac{eQ}{\hbar}\right)^2 J_{00}(2\omega_0)$$

$$R_{2f} = \left(\frac{eQ}{\hbar}\right)^2 [J_{00}(0) + J_{00}(\omega_0)]$$

$$R_{2s} = \left(\frac{eQ}{\hbar}\right)^2 [J_{00}(\omega_0) + J_{00}(2\omega_0)] \quad (1)$$

where e is the electronic charge, $\hbar$ is the reduced Planck constant, and ω_0 and Q are the nuclear Larmor frequency and quadrupole moment.

$J_{00}(\omega)$ is proportional to the Fourier transform of the autocorrelation function of the Oth irreducible component of the fluctuating EFG V_0. However, to reduce the errors involved in the calculation of $J_{00}(\omega)$ by MD simulations, it is better to derive it from the whole EFG tensor,[32] to which it is proportional in isotropic systems:[33]

$$J_{00}(\omega) = \frac{1}{60}\langle \mathbf{V}(0):\mathbf{V}(0)\rangle \int_{-\infty}^{\infty} \cos(\omega t) G(t)\, dt \quad (2)$$

where $G(t)$ is the normalized autocorrelation function of the EFG tensor:

$$G(t) = \frac{\langle \mathbf{V}(0):\mathbf{V}(t)\rangle}{\langle \mathbf{V}(0):\mathbf{V}(0)\rangle} \quad (3)$$

$$\langle \mathbf{V}(0):\mathbf{V}(t)\rangle = \sum_{k=-2}^{2} (-1)^k \langle V_k(0) V^*_{-k}(t)\rangle \quad (4)$$

V_k's are the irreducible components of the EFG in the laboratory frame:

$$V_0 = \frac{\sqrt{6}}{2} V_{zz}$$

$$V_{\pm 1} = \mp (V_{xz} \pm i V_{yz})$$

$$V_{\pm 2} = \frac{1}{2}(V_{xx} - V_{yy} \pm 2i V_{xy}) \quad (5)$$

V_{ij} are the second partial derivatives of the electric potential V at the nuclear site in the laboratory frame.

It is common practice to group the constants in eqs 1 and 2 into a single constant, the quadrupolar coupling constant χ, defined as

$$\chi^2 = \frac{2}{3}\left(\frac{eQ}{h}\right)^2 \langle \mathbf{V}(0):\mathbf{V}(0)\rangle \quad (6)$$

For interpreting the experimental data of charged macromolecules in solution, the observed $J(\omega)$'s are usually fitted to a sum of Lorentzian functions, assuming that each of them is related either to a time-scale separated process which randomizes the EFG and/or to a fast exchange of nuclei distributed over different sites.[34] This is equal to assuming that the electric field gradient time correlation function (EFGTCF) decays as a sum of exponential functions:

$$\left(\frac{eQ}{\hbar}\right)^2 J_{00}(\omega) = \frac{\pi}{10}\chi^2 \int_{-\infty}^{\infty} \cos(\omega t) G(t)\, dt = \frac{\pi}{10}\sum_{i=1}^{N} \chi_i^2 \int_{-\infty}^{\infty} \cos(\omega t) e^{-|t|/\tau_i}\, dt \quad (7)$$

If the correlation times characterizing $G(t)$ are small compared to the Larmor frequency ($\omega_0 \tau \ll 1$), all of the relaxation rates in eqs 1 become equal and this condition is called the extreme narrowing regime. By combining eqs 1, 2, and 6, the relaxation rates can be written as

$$R = \frac{2}{5}\pi^2 \chi^2 \int_0^{\infty} G(t)\, dt \quad (8)$$

As to the origin of the EFG at the nuclear site, several theories have been formulated in order to understand the relaxation mechanism at a microscopic level. The electrostatic theories[35−37] ascribe the EFG to the charges and dipole moments of the particles surrounding the nucleus, with the electron cloud of the quadrupolar atom mediating the EFG at the nuclear site. The electronic theory[38] ascribes the EFG to the distortion of the electron cloud of the quadrupolar nucleus due to collisions with neighboring particles. In the earliest computational studies of the quadrupolar relaxation of monatomic ions in dilute aqueous solution,[39] the EFG at the nuclear site was calculated both quantum chemically, thus taking into account all possible origins of the EFG, and by classical electrostatics. In the latter treatment, the effect of the electron cloud on the EFG was accounted for by a polarization factor, the Sternheimer factor $(1 + \gamma_\infty)$, which acts as an amplifier of the externally generated EFG ($\mathbf{V}_{ext}$):

$$\mathbf{V} = (1 + \gamma_\infty)\mathbf{V}_{ext} \quad (9)$$

Comparison of the results by the two treatments revealed that for large monovalent ions the electrostatic treatment was in good agreement with the more rigorous quantum chemical approach. Since then, the relaxation mechanism of several monatomic quadrupolar nuclei in simple or heterogeneous systems has been investigated by molecular dynamics simulation employing the Sternheimer approximation.[26−30,32,40] Of particular relevance to our study on the ^{23}Na quadrupolar relaxation in DNA aqueous solution are the all-atoms MD studies in complex systems.[28,29] These studies indicated that simplification of the model system beyond the atomistic scale (e.g., the use of a continuum model for the solvent) cannot adequately reproduce the EFG since this quantity was found to be highly dependent on the local hydration structure and the solvent contribution to the total EFG is not easily predictable.

3. Results and Discussion

In this section, we first describe in detail the interactions between DNA and sodium ions observed from 1 to 8 ns of the MD production run. Next the quadrupolar magnetic relaxation of ^{23}Na is analyzed, starting with a general picture of the EFGTCF decay; then we study the dependence of the relaxation on the distance of the quadrupolar ion from the DNA surface. Getting into deeper detail, we show how different binding sites affect the relaxation parameters of the bound ion.

3.1. Na/DNA Interactions. During the course of the simulation, several types of interaction between sodium ions and DNA were observed, including direct or water-mediated binding to the grooves or to the phosphates. In this section, we discuss

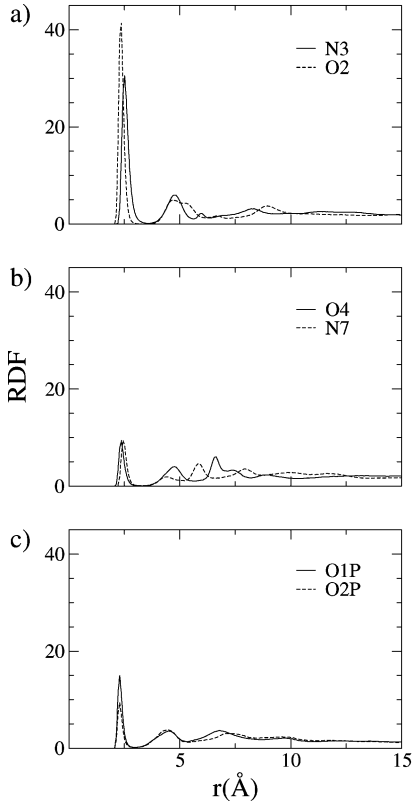

Figure 1. RDFs between Na^+ and selected atoms on DNA: (a) in the minor groove (adenine N3 and thymine O2), (b) in the major groove (adenine N7 and thymine O4), and (c) in the backbone (phosphate's oxygens). Only A·T base pairs were included in the analysis.

the distribution of sodium ions around DNA in terms of the radial distribution functions (RDFs) between Na^+ and selected electronegative or charged atoms in the minor and major grooves and in the backbone (Figure 1). The analysis of the RDFs is supplemented with the spatial distribution functions (SDFs) of the ion and water atoms around DNA for selected binding modes (Figure 2). For each mode, the SDFs have been calculated during the binding event, in a local reference system the origin of which is at the atom bound to the ion (A1); the axes are defined by means of two vectors connecting A1 to two appropriate atoms, A2 and A3 (see Figure 2 for details).

In all of the RDFs, the first peak corresponds to the direct binding of sodium to DNA; from the relative intensities, it is seen that this binding is more favored in the region of the minor groove than in other sites on the DNA surface. In fact, a sodium ion intrudes into the minor groove from the very beginning of the equilibration step, replacing a water molecule of the first layer of the hydration spine, a peculiar structural motif found in A-tracts;[7,14,41−43] this replacement is apparent in the SDFs displayed in Figure 2a. This intrusion is revealed not only by the strong intensity of the first peak of the RDFs between Na^+ and the atoms of the minor groove (RDF-minor) but also by the peaks at 5.9 and 6.5 Å of the RDFs between Na^+ and the atoms N7 and O4 in the major groove (RDF-major). Other intrusions into the first hydration layer of the minor groove contribute to the first peak of RDF-minor: simultaneous direct binding to N7 and O4′ of adenine is observed in the trajectory (duration, ca. 0.5 ns); as shown in Figure 2c, this kind of intrusion leads to the disruption of the hydration spine and to the widening of the minor groove as observed in a previous simulation.[22]

The first peak in the RDF-major originates from several direct bindings of Na^+ to the thymine O4 (duration, up to 0.3 ns) and from a single direct binding to the adenine N7 (duration, ca. 2 ns); the corresponding SDFs are shown in Figure 2b,d. The hydration structure around the ion is definitely more ordered when the ion is bound to the adenine, with an octahedral coordination in which three water molecules bridge the ion to DNA's electronegative atoms of adjacent base pairs and to the phosphate (thymine O4, phosphate O2, and adenine N7).

As witnessed by the RDF between the ion and the atoms O1 or O2 of the phosphate group (RDF-phosphate), direct binding to the oxygens is observed also in the backbone region, the oxygen facing the minor groove (O1) being the most favored. The SDF displayed in Figure 2g reveals that one sodium ion replaces one of the water molecules hydrating the phosphate oxygen. In other cases (not shown), the ion moves from one hydration site to another of the same oxygen or from one oxygen to the other; however in no case does the coordination involve both of the oxygens.

The second peak in either RDF-minor or RDF-major originates not only from solvent separated ions but also from ions bound to adjacent base pairs. Either in the major groove or in the widened central region of the minor groove, fully hydrated ions can maintain the same relative position to the DNA bases up to several hundreds of picoseconds; examples of SDFs are reported in Figure 2e (minor groove) and Figure 2f (major groove).

The second peak of the RDF-phosphate originates from solvent separated ions or from the ion bound to N7 in the major groove.

The remaining peaks in all of the RDFs result from direct binding of the ion either to nearby phosphates or to the bases in both grooves.

Finally we note that the displayed angularly averaged RDFs somehow hide the relative proportion of ions directly or indirectly bound; therefore this quantity was calculated separately, revealing that the absolute number of ions is almost the same (ca. 4 ions) in the two regions.

3.2. Analysis of the Electric Field Gradient. 3.2.1. Time Correlation Functions. The calculation of the EFGTCF of sodium ions in DNA aqueous solution (DS) was carried out with a time resolution of 0.1 ps over the range 1−8 ns, while in the dilute aqueous solution of sodium chloride (AS), because of the faster EFGTCF decay, a resolution of 0.01 ps was chosen and the calculation was performed over 800 ps.

Figure 3a shows the normalized EFGTCF of Na^+ in DS calculated either taking into account all of the ions in the system or excluding the ion residing in the minor groove for the whole simulation run.

It can be seen that the complete randomization of the EFGTCF when all of the ions are taken into consideration requires several nanoseconds. Comparison of the two curves in Figure 3a indicates clearly that such a slow randomization is due to the ion bound to the minor groove for the entire simulation; in fact, if this ion is excluded from the calculation of the EFGTCF a much faster decay is observed and the complete randomization is reached in ca. 2 ns.

Previous MD simulations[21,22,24,44] and experimental data[13] suggested that water replacement by sodium ions in the minor groove of A-tracts is only partial, ca. 5% according to the NMR estimate; hence including the trapped ion in the calculation leads to an overwhelming estimate of its contribution to the total EFGTCF. Accordingly, in the following we have excluded this ion from the EFGTCF calculation.

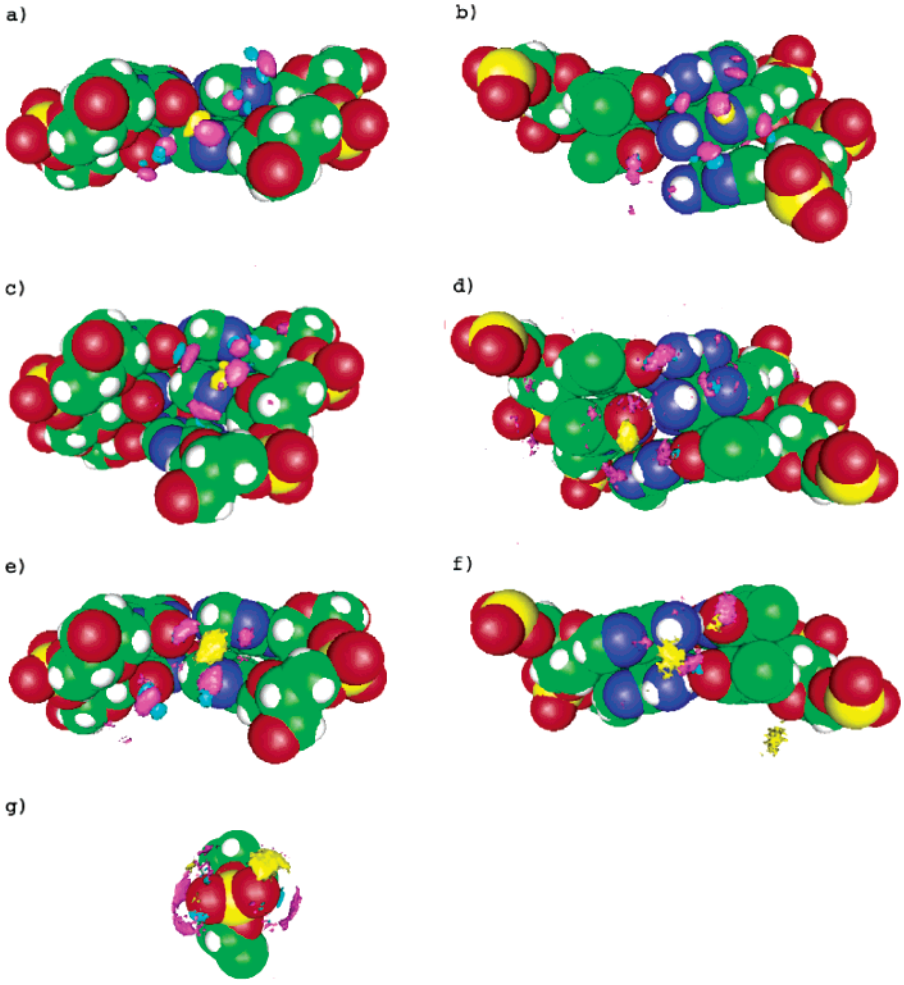

Figure 2. SDFs of Na^+ (yellow), water's oxygen (violet), and hydrogen (cyan) around DNA during selected Na^+−DNA binding events. (a) Direct binding to adenine N3 and thymine O2 (7 ns); A18-N3, A19-N3, T2-O2. (b) Direct binding to adenine N7 (2 ns); A8-N7, A7-N7, T13-O4. (c) Direct binding to adenine N3 and O4′ (0.5 ns); A8-N3, A7-N3, A8-O4′. (d) Direct binding to thymine O4 (0.25 ns); A16-N6, A17-N6, T5-O4. (e) Solvent-mediated binding in the minor groove (1 ns); T13-O2, T14-O2, A8-N3. (f) Solvent-mediated binding in the major groove (0.5 ns); A16-N6, A17-N6, T5-O4. (g) Direct binding to phosphate's oxygen (0.4 ns); T3-P, T3-O1P, T3-O2P. Numbers in parentheses indicate the time length over which the SDF and the average structure were calculated, while the three residue and atom names label the atoms A1, A2, and A3 defining the reference system.

As can be seen in Figure 3a for DS and in Figure 4a for SA, the EFGTCFs are definitely nonexponential. Assuming for the decay the following functional form,

$$G(t) = \sum_{i=1}^{N} a_i e^{-t/\tau_i} \tag{10}$$

we found that the best fits were obtained using 3 and 5 exponentials for SA and DS, respectively. The best fit values of the time constants, τ_i, are reported in Table 1 with their associated errors; the latter are standard deviations calculated from the averages over 250 ps separate segments of the MD trajectory in AS and over 4 ns partially overlapping segments in DS.

In AS, the slow part of the decay is not reproduced correctly by a 2-exponential fit, Figure 4b, while in DS the 4-exponential fit fails to reproduce either the initial part or the tail of the EFGTCF, Figure 3b. On the other side, no improvement is gained by increasing the number of exponentials: 3- and 4-exponential fits in SA are almost completely superimposed, and the same holds true in DS for 5- and 6-exponential fits.

The nonexponential behavior of the EFGTCF of ^{23}Na in simple electrolyte aqueous solution has already been observed in previous computational studies,[40,45] where the fit to a sum of exponentials was limited to two terms with correlation times of ca. 0.1−0.15 ps and ca. 1−1.5 ps consistent with the values of 0.06 and 1.2 ps that we obtained with a 2-exponential fit. These correlation times were found to be shorter than any single particle correlation time, and their origin was attributed to the cooperative dynamics of the molecules in the solvating shell of the ion which led to a partial static and dynamical quenching of the EFG.

The comparison of the correlation times of the EFGTCFs obtained in DS and in AS evidences that the three shortest time constants in DS reflect motional dynamics similar to those probed by the sodium ion in dilute aqueous solution. One of the remaining time constants, ca. 70 ps, is (at the common magnetic field strengths and temperatures) in the extreme narrowing regime, a condition where no information can be obtained on the shape of the EFGTCF from NMR experiments; on the contrary, the longest time constant is outside this regime and thus can be compared to the experimental measures.

In a recent investigation of some DNA oligomers containing A-tracts, Denisov and Halle[13] have used ^{23}Na NMR dispersion experiments to obtain the spectral densities as a function of the magnetic field strength. These quantities were then fitted to a

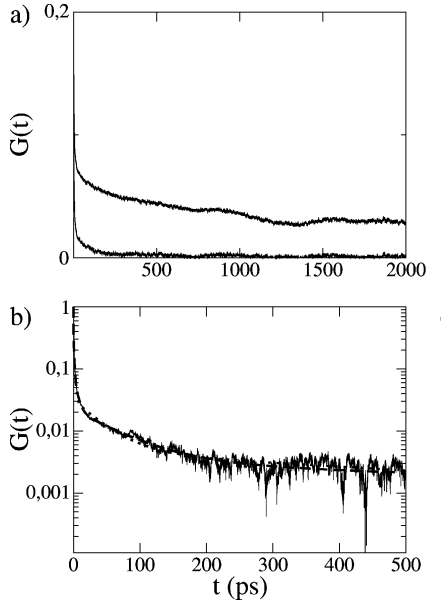

Figure 3. (a) Normalized EFGTCFs in the DNA solution calculated including all of the ions (upper curve) or excluding the ion stuck in the minor groove (lower curve). (b) Logarithmic plot of the normalized EFGTCF calculated excluding the stuck ion (continuous line), 4-exponential fit (dotted line) and 5-exponential fit (dashed line).

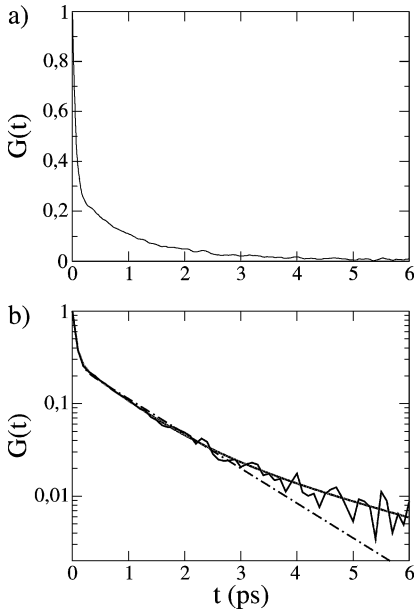

Figure 4. (a) Normalized EFGTCF in NaCl dilute aqueous solution. (b) Logarithmic plot of the normalized EFGTCF (continuous line), biexponential fit (dash dotted line) and 3-exponential fit (continuous line).

TABLE 1: Fits of the Normalized EFGTCF to a Linear Combination of Exponential Functions[a]

	τ_1	τ_2	τ_3	τ_4	τ_5
AS	0.055 ± 0.001	0.88 ± 0.1	3.2 ± 2		
DS	0.051 ± 0.001	1.0 ± 0.1	5.0 ± 1	66 ± 25	1200 ± 500

[a] τ in ps.

sum of Lorentzian functions and a constant term. They assigned the Lorentzian with the longest correlation time to the ions bound in the minor groove for times longer than the tumbling time, which in the present work has been excluded from the analysis of the EFG. The other correlation times were scaled to 298 K and H_2O as solvent, using the equality $\tau_1 = \tau_2(\eta_1/T_1)$-$(T_2/\eta_2)$ (where τ's, η's, T's are the correlation times, viscosities, and temperatures in two different experimental conditions) obtained from the famous Einstein relation; the scaled values ranged from 0.4 to 2.4 ns, in pretty good agreement with the value of 1.2 ns found in the present simulation.

TABLE 2: ^{23}Na Relaxation Constants at 100 MHz[a]

	R_{1f}	R_{1s}	R_{2f}	R_{2s}
H_2O, 298 K	44	32	51	38
D_2O, 277 K	70	55	112	63

[a] R_i in s^{-1}.

TABLE 3: Dependence of the Quadrupolar Coupling Constant on the Distance from the DNA Surface[a]

	distance (Å)					
	<3	3−4	4−5	5−6	6−7	7−8
χ	2.13±0.06	2.01±0.6	1.97±0.04	1.99±0.04	1.98±0.07	1.98±0.06

[a] χ in MHz.

With the relaxation parameters obtained by the MD simulation, we have calculated using eqs 1, 7, and 10 the ^{23}Na relaxation rates which we reported in Table 2. For purpose of comparison with the experimental values, we also report the relaxation rates obtained by scaling the τ_i's to 277 K in D_2O solution. In these conditions, Denisov and Halle[13] found values of $R_{1f,s}$ and R_{2s} in the range of 100−150 s^{-1} and ca. 280 s^{-1} for R_{2f} at 100 MHz. Though these rates are larger than those obtained in the present simulation, there is a good qualitative agreement, specially if one considers that our estimates are lower limits to the "true" values, because of the exclusion of the stuck ion from the EFG calculation. On the other hand, if this ion is taken into account, the relaxation rates increase by a factor ranging from 5 to 20 depending on the relaxation component, leading to the limit value of 4600 s^{-1} in the extreme narrowing condition, definitely too much larger than the experimental measures. Due to these and the previous considerations, we infer that the occupancy of ions in the minor groove with residence time of several nanoseconds should be smaller than what is indicated by the MD simulation.

3.2.2. Dependence on the Distance from DNA. In this section, we discuss the dependence of the dynamical and static quadrupolar relaxation parameters of ^{23}Na on the distance from the DNA surface. These studies are relevant to the analysis of the experimental ^{23}Na relaxation data, which are usually interpreted in the framework of the Manning condensation theory and a two-state model in which ions exchange rapidly between a "bound" and a "free" state rather loosely defined. According to this theory, the condensed or bound ions are considered to be territorially bound within about 7 Å from the DNA surface.[2,46]

In Table 3, we report the quadrupolar coupling constants calculated as a function of the distance between Na^+ and the closest DNA atom, over the whole production run; the estimated errors are the standard deviations of subaverages obtained from 100 ps portions of the MD.

As shown in Table 3, the quadrupolar coupling constant is slightly larger than the bulk value only when the ion is directly bound to DNA (distances < 3 Å), while it is almost constant at longer distances. Though, in view of the highly charged nature of DNA, this result may appear surprising, we point out that in a previous computational study on the ^{23}Na quadrupolar relaxation in a system containing a hydrated sodium dimethyl phosphate, Chen and Rossky[30] calculated individual contributions to the total $\langle V^2 \rangle$ and concluded that "the counteranion charge produces a large EFG at the sodium ion as well as an

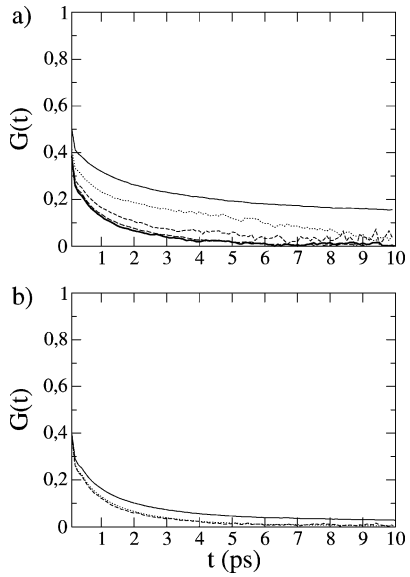

Figure 5. (a) Normalized EFGTCFs for sodium ions in regions at increasing distance from the DNA surface. Spatial regions from 2 to 3 Å (continuous line), from 3 to 4 Å (dotted line), from 4 to 5 Å (dashed line), from 5 to 7 Å (long-dashed line), from 6 to 8 Å (continuous bold line), from 7 to 9 Å (dotted bold line), beyond 14 Å (dashed bold line). (b) Normalized EFGTCFs due to all of the ions except the one stuck in the minor groove (continuous line), ions beyond 3.8 Å (dotted line), and ions beyond 6 Å (dashed line).

indirect polarization of the solvent molecules, with a net contribution very comparable to that in which no counterionic charge and polarity are present".

The EFGTCFs calculated in regions of the system at various distances from the DNA surface are reported in Figure 5a. The thickness of the layers varied from 1 to several angstroms depending on the distance from the DNA surface; in regions where the ions remained for several picoseconds, it was possible to study the EFGTCF for 10 ps in layers 1 Å thick; on the contrary, in regions beyond 5 Å from the surface the EFGTCF profile is too noisy, when calculated on a layer of 1 Å, to allow any useful information to be extracted after a few picoseconds and accordingly the thickness was increased. As can be seen in Figure 5a, the profiles of the EFGTCF became virtually identical at ca. 6 Å, so that this limiting distance can be taken as an operative definition of the bound state in the NMR sense. This result implies that the "NMR bound ions" are those either directly bound to DNA atoms or separated by a single water molecule. Incidentally, we notice that this value agrees nicely with the radius of 7 Å from the DNA surface assumed by Manning.

The experimentally observed relaxation rates are population-weighted averages over the ionic distribution in the entire system. To assess the contribution of directly bound ions to the total relaxation rates, we have compared the all-ion EFGTCF with the time correlation functions calculated excluding ions either within 3.8 Å from the surface or within 6 Å, Figure 5b. In the former case, the longest correlation time constant obtained from the fit of the EFGTCF to a 3-exponential function is ca. 10 ps (the fit does not improve by increasing the number of exponentials), much shorter than those found in oligomeric DNA solution. Since the two longest time constants of the all-ion EFGTCF are missing when the ions directly bound to DNA are excluded from the EFG calculation, we infer that they must pertain to motional processes occurring in the vicinity of these ions.

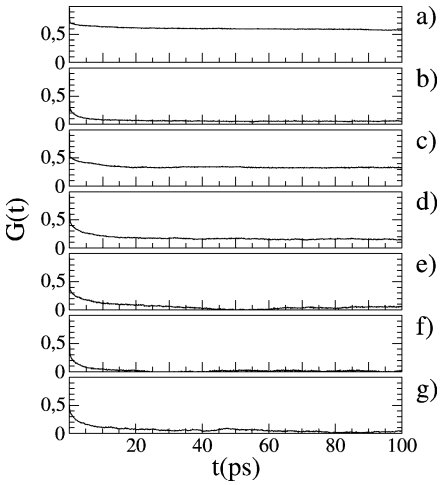

Figure 6. Normalized EFGTCFs of selected ions bound to DNA in different sites calculated during the binding event. The order of the plots is the same as in Figure 2.

Figure 5a shows that the EFGTCF of ions separated from the DNA surface by a water molecule is affected by the oligomer; therefore the overlapping of the EFGTCFs calculated excluding ions within 3.8 and 6 Å is related to the low occupancy of long-lasting sodium ions in the secondary hydration layer relative to that beyond 6 Å. The latter implication prompted to us the question of whether the distribution of ions around DNA was in thermal equilibrium or not. In fact, separate 1 ns segments of simulation provided almost identical relaxation times for ions beyond 3.8 Å from the DNA surface, so that it was concluded that the system was in thermal equilibrium.

3.2.3. Dependence on the Binding Site. Ions can bind, either directly or through a water molecule, to atoms in the grooves or in the backbone of the double helix. In this section, we investigate the effects of the binding on the quadrupolar coupling constant and on the EFGTCF.

In Figure 6, we display the ^{23}Na EFGTCFs calculated during the binding events shown in Figure 2, while the corresponding χ's are collected in Table 4 together with the standard deviations of subaverages calculated on separate 100 ps segments of the MD.

The EFGTCFs of ions directly bound to the minor groove, Figure 6a,c, decay slower than in any other binding site. This behavior is likely related to the motions of water molecules surrounding the ions which are reasonably hampered in the narrow minor groove. In fact, the decay is faster when the ion disrupts the hydration spine and widens the groove, Figure 6c, rather than when it replaces a water molecule of the hydration spine, narrowing the groove, Figure 6a. The EFGTCFs of ions bound via a water molecule to the minor groove, Figure 6e, or to the major groove, Figure 6f, decorrelate faster than those of directly bound ions, the decay being faster in the major groove.

The quadrupolar coupling constants vary from 1.8 to 2.6 MHz, depending on the binding site. These values fall in the range of 1−5 MHz found by solid-state ^{23}Na NMR for ions bound to oxygens in silicates, alumino silicates, and other compounds.[47]

The quadrupolar coupling constant in most of the binding sites is close to that in the bulk (χ = 1.98 MHz); however marked differences are observed either when the sodium ion replaces a water molecule of the hydration spine (χ = 2.59 MHz) or when it is bound to one of the sites in the major groove (χ = 1.77 MHz). These differences can be rationalized when looking at the coordination geometry around the ion: the ion

TABLE 4: Quadrupolar Coupling Constant at Specific Binding Sites[a]

	a	b	c	d	e	f	g
χ	2.59 ± 0.14	1.77 ± 0.06	2.07 ± 0.09	2.19 ± 0.08	1.96 ± 0.06	1.94± 0.06	2.16 ± 0.09

[a] The letters are the same as in Figure 2. χ in MHz.

residing in the major groove is six coordinated with a pretty regular octahedral symmetry, Figure 2b, while the ion in the minor groove is five coordinated, Figure 2a, and therefore has a lower symmetry and higher electric field gradient.

4. Conclusions

The microscopical description obtained by classical molecular dynamics simulation allowed us to obtain several details on the effects of DNA on the ^{23}Na quadrupolar relaxation which are of importance in the interpretation of the experimental data obtained by ^{23}Na NMR.

The present simulation shows that the polyion affects the quadrupolar relaxation of sodium ions within 6 Å from its surface, a distance rather close to the Manning radius. These effects show up mainly in the dynamics of the EFG, which for ions directly bound to DNA is slower than in the bulk, particularly at those sites where the motion of the hydrating water is hampered by steric hindrance. The EFG decay is slowed also when the ions are bound through a water molecule, though to a lesser extent than for direct binding.

The quadrupolar coupling constant changes significantly, compared to the bulk value, only in a few types of direct binding, depending on the particular coordination geometry at the ion site; however in the majority of direct contacts the quadrupolar coupling constant remains rather close to the value in the bulk. Finally, when the ion is bound to DNA through a solvent molecule, the coupling constant is definitely as that in the bulk.

The calculated relaxation rates are consistent with recent experimental data on DNA oligomers, and the speed-up of the ^{23}Na relaxation rate, compared to simple electrolyte solution, is mainly due to the contribution of ions directly bound to the surface of the oligomer.

Comparing the relaxation rates calculated either including all the ions in the simulation box or excluding an ion trapped in the minor groove for the whole dynamics reveals that the sodium occupancy at the minor groove of A-tracts is much smaller than 100%. In this context, we would like to stress that the calculation of the relaxation parameters of quadrupolar nuclei can be an easy and virtually not computationally demanding method to cross-check the MD simulation when quadrupolar counterions are part of the system.

5. Methods

The simulation aims to mimic an isotropic aqueous solution of a DNA oligomer in minimal salt condition, at constant temperature (298 K) and constant pressure (1 bar); the system comprises one flexible DNA duplex, CT_4A_4G, 18 Na^+ neutralizing counterions, and 3800 water molecules.

The AMBER force field parameters were used for the DNA decamer,[48,49] the SPC flexible water model was used for the solvent,[50] and the Dang and Smith parameters[51] were used for the sodium ions. The double time step algorithm by Tuckerman et al.[52] was used with a time step of 0.2 fs for short-ranged (cutoff = 5.Å) intra- and intermolecular interactions and a time step of 2.0 fs for the others (cutoff = 14.Å).

The simulation was carried out in a truncated octahedral box of length ca. 62 Å, with periodic boundary conditions and the minimum image convention.

The Ewald method was employed for the treatment of long-range electrostatic interactions.[53] In the real space, the cutoff radius was $R_{cut} = 14$ Å, while the cutoff radius in the reciprocal space, k_{max}, was determined from the condition $\exp(-\alpha^2 k_{max}^2/(R_{cut}\alpha)^2) = \exp(-8.)$; the screening parameter α was taken as $\alpha R_{cut} = 2.7$. These parameters provide a relative precision of $\exp(-8.) \sim \mathrm{erfc}(2.7) \sim 10^{-4}$ for both the reciprocal and the real space terms of the Ewald sum. System setup, equilibration, and production runs are as described in Lyubartsev and Laaksonen.[20] Specifically, the starting canonical B-DNA oligomer was placed along the *Z*-axis of the simulation cell. The water molecules were located initially on a cubic lattice with random orientation out of a cylinder of radius 12 Å coaxial with DNA. Ions were distributed randomly among the water molecules. During the first 100 ps of simulation, DNA was kept fixed, allowing the water and ions to equilibrate, and after this stage all the atoms in DNA were allowed to move. The system was further equilibrated during the next 900 ps, whereafter the production run was started. Temperature and pressure were regulated by the Nosé-Hoover thermostat and barostat[54] using time constants of 30.0 and 700.0 fs for thermal and volume fluctuations, respectively.

For comparison purposes, we also studied a simple dilute electrolyte aqueous solution comprising 400 SPC flexible water molecules, 1 Na^+ and 1 Cl^-, in the same physical conditions as in the DNA simulation. The simulations were carried out using a version of the Mdyna*mix* program,[55] modified to accommodate the calculation of the components of the EFG at every nucleus during the simulation. The total EFG is assumed to be pairwise additive,[56] and its calculation was completely included into the Ewald summation scheme.

Fits of the EFGTCF were done using a few subroutines of an in-house-made program (http://www.fos.su.se/baltzar/APME/) based on the Newton−Raphson minimization algorithm.

SDFs were calculated by the analysis program TRANAL accompanying the Mdyna*mix* software and displayed using the gOpenMol software.[57,58] The intensity levels (i.e., the probability to find an atom in a certain point around DNA compared to the bulk value) are the same in all the SDFs shown in Figure 2: 10 for H and O of water, 1000 for Na^+.

Acknowledgment. This project was financially supported by the Swedish Science Council and by the "Progetto Giovani Ricercatori" of the University of Cagliari. F.M. thanks Baltzar Stevensson for his assistance in the use of the APME program and for stimulating discussions and Flaminia Cesare Marincola for her helpful comments.

References and Notes

(1) Nordenskiöld, L.; Chang, D.; Anderson, C.; Record, M. J. *Biochemistry* **1984**, *23*, 4309−4317.

(2) Braunlin, W. H. *Adv. Biophys. Chem.* **1995**, *5*, 89−139.

(3) van Dijk, L.; Gruwel, M.; Jesse, W.; De Bleijser, J.; Leyte, J. *Biopolymers* **1987**, *26*, 261−284.

(4) Cesare Marincola, F.; Casu, M.; Saba, G.; Lai, A. *ChemPhysChem* **2001**, *67*, 569−575.

(5) Cahen, P.; Luhmer, M.; Fontaine, C.; Morat, C.; Reisse, J.; Bartik, K. *Biophys. J.* **2000**, *78*, 1059−1069.
(6) Tereshko, V.; Minasov, G.; Egli, M. *J. Am. Chem. Soc.* **1999**, *121*, 3590−3595.
(7) Shui, X.; McFail-Isom, L.; Hu, G.; Williams, L. *Biochemistry* **1998**, *37*, 8341−8355.
(8) Shui, X.; Sines, C. C.; McFail-Isom, L.; VanDerveer, D.; Williams, L. *Biochemistry* **1998**, *37*, 16877−16887.
(9) Sines, C. C.; McFail-Isom, L.; Howerton, S.; VanDerveer, D.; Williams, L. *J. Am. Chem. Soc.* **2000**, *122*, 11048−11056.
(10) McFail-Isom, L.; Sines, C.; Williams, L. D. *Curr. Opin. Struct. Biol.* **1999**, *9*, 298−304.
(11) Soler-Lopez, M.; Malinina, L.; Liu, J.; Huynh-Dinh, T.; Subirana, J. *J. Biol. Chem.* **1999**, *274*, 23683−23686.
(12) Hud, N. V.; Sklenar, V.; Feigon, J. *J. Mol. Biol.* **1999**, *286*, 651−660.
(13) Denisov, V.; Halle, B. *Proc. Natl. Acad. Sci. U.S.A.* **2000**, *97*, 629−633.
(14) Young, M. A.; Jayaram, B.; Beveridge, D. *J. Am. Chem. Soc.* **1997**, *119*, 59−69.
(15) Auffinger, P.; Westhof, E. *J. Mol. Biol.* **2000**, *300*, 1113−1131.
(16) Auffinger, P.; Westhof, E. *J. Mol. Biol.* **2001**, *305*, 1057−1072.
(17) Bonvin, A. *Eur. Biophys. J.* **2000**, *29*, 57−60.
(18) Feig, M.; Pettitt, B. M. *Biophys. J.* **1999**, *77*, 1769−1781.
(19) Howerton, S.; Sines, C.; VanDerveer, D.; Williams, L. *Biochemistry* **2001**, *40*, 10023−10031.
(20) Lyubartsev, A. P.; Laaksonen, A. *J. Biomol. Struct. Dyn.* **1998**, *16*, 579−592.
(21) McConnell, K.; Beveridge, D. *J. Mol. Biol.* **2000**, *304*, 803−820.
(22) Mocci, F.; Saba, G. *Biopolymers* **2003**, *68*, 471−485.
(23) Štefl, R.; Koča, J. *J. Am. Chem. Soc.* **2000**, *122*, 5025−5033.
(24) Hamelberg, D.; McFail-Isom, L.; Williams, L.; Wilson, W. *J. Am. Chem. Soc.* **2000**, *122*, 10513−10520.
(25) Hamelberg, D.; Williams, L.; Wilson, W. *J. Am, Chem. Soc.* **2001**, *123*, 7745−7755.
(26) Odelius, M.; Laaksonen, A. Combined MD simulation and NMR relaxation studies of molecular motion and intermolecular interactions. In *Molecular Dynamics. From Classical to Quantum Methods*; Balbuena, P., Seminario, J., Eds.; Theoretical and Computational Chemistry, Vol. 7; Elsevier Science: Amsterdam, 1999.
(27) Reddy, M.; Rossky, P.; Murthy, C. *J. Phys. Chem.* **1987**, *91*, 4923−4933.
(28) Forester, T. *Mol. Phys.* **1991**, *73*, 1335−1347.
(29) Linse, P.; Halle, B. *Mol. Phys.* **1989**, *67*, 537−573.
(30) Chen, S.; Rossky, P. *J. Phys. Chem.* **1993**, *97*, 10803−10812.
(31) Hubbard, P. S. *J. Chem. Phys.* **1970**, *53*, 985−987.
(32) Schnitker, J.; Geiger, A. *Z. Phys. Chem.* **1987**, *155*, 29−54.
(33) Hubbard, P. *Phys. Rev.* **1969**, *180*, 319−326.
(34) Mulder, C.; De Bleijser, J.; Leyte, J. *Chem. Phys. Lett.* **1979**, *69*, 354−358.
(35) Valiev, K. *Sov. Phys. JETP* **1960**, *37*, 77−82.
(36) Hertz, H. *Ber. Bunsen-Ges. Phys. Chem.* **1973**, *77*, 531−540.
(37) Versmold, H. *Mol. Phys.* **1986**, *57*, 201−216.
(38) Deverell, C. *Mol. Phys.* **1969**, *16*, 491−500.
(39) Engström, S.; Jönson, B.; Jönsson, B. *J. Magn. Reson.* **1982**, *50*, 1−20.
(40) Roberts, J.; Schnitker, J. *J. Phys. Chem.* **1993**, *97*, 5410−5417.
(41) Drew, H.; Dickerson, R. *J. Mol. Biol.* **1981**, *151*, 535−556.
(42) Chuprina, V.; Heinemann, U.; Nurislamov, A.; Zielenkiewicz, P.; Dickerson, R. E. *Proc. Natl. Acad. Sci. U.S.A.* **1991**, *88*, 593−597.
(43) Feig, M.; Pettitt, B. M. *J. Mol. Biol.* **1999**, *286*, 1075−1095.
(44) Madhumalar, A.; Bansal, M. *Biophys. J.* **2001**, *85*, 1805−1816.
(45) Engström, S.; Jönsson, B.; Impey, R. *J. Chem. Phys.* **1984**, *80*, 5481−5486.
(46) Manning, G. *Q. Rev. Biophys.* **1978**, *2*, 179−246.
(47) Freude, D. Quadrupolar Nuclei in Solid-state Nuclear Magnetic Resonance. In *Encyclopedia of Analytical Chemistry*; Meyers, R. A., Ed.; J. Wiley: Chichester, 2000.
(48) Cornell, W.; Cieplak, P.; Bayly, C.; Gould, I.; Merz, K. J.; Ferguson, D.; Spellmeyer, D.; Fox, T.; Caldwell, J.; Kollmann, P. *J. Am. Chem. Soc.* **1995**, *117*, 5179−5197.
(49) Cheatham, T. I.; Cieplak, P.; Kollmann, P. *J. Biomol. Struct. Dyn.* **1999**, *16*, 845−862.
(50) Toukan, K.; Ramhan, A. *Phys. Rev. B* **1985**, *31*, 2643−2648.
(51) Dang, L.; Smith, D. *J. Chem. Phys.* **1993**, *99*, 6950−6956.
(52) Tuckerman, M.; Berne, B.; Martyna, G. *J. Chem. Phys.* **1983**, *97*, 1990−2001.
(53) Allen, M.; Tildesley, M. *Computer simulation of liquids*; Clarendon Press: Oxford, 1987.
(54) Melchionna, S.; Ciccotti, G.; Holian, B. *Mol. Phys.* **1993**, *78*, 533.
(55) Lyubartsev, A. P.; Laaksonen, A. *Comput. Phys. Commun.* **2000**, *128*, 565−589.
(56) Engström, S.; Jönsson, B. *Mol. Phys.* **1981**, *43*, 1235−1253.
(57) Laaksonen, L. *Mol. Graph.* **1992**, *10*, 33−34.
(58) Bergman, D.; Laaksonen, L.; Laaksonen, A. *J. Mol. Graphics Modell.* **1997**, *5*, 301−306.